Donnan Permselectivity in Layer-by-Layer Self-Assembled Redox Polyelectrolye Thin Films

Ernesto J. Calvo* and Alejandro Wolosiuk

Contribution from INQUIMAE, Departamento de Química Inorgánica, Analítica y Química Física, Facultad de Ciencias Exactas y Naturales, Pabellón 2 Ciudad Universitaria, AR-1428 Buenos Aires, Argentina

Received January 22, 2002

Abstract: Redox polyelectrolyte multilayers have been assembled with use of the layer-by-layer (LBL) deposition technique with cationic poly(allylamine) modified with Os(bpy)$_2$ClPyCHO (PAH-Os) and anionic poly(styrene)sulfonate (PSS) or poly(vinyl)sulfonate (PVS). Different behavior has been observed in the formal redox potential of the Os(II)/Os(III) couple in the polymer film with cyclic voltammetry depending on the charge of the outermost layer and the electrolyte concentration and pH. The electrochemical quartz crystal microbalance (EQCM) has been used to monitor the exchange of ions and solvent with the external electrolyte during redox switching. At low ionic strength Donnan permselectivity of anions or cations is apparent and the nature of the ion exclusion from the film is determined by the charge of the topmost layer and solution pH. At high electrolyte concentration Donnan breakdown is observed and the osmium redox potential approaches the value for the redox couple in solution. Exchange of anions and water with the external electrolyte under permselective conditions and salt and water under Donnan breakdown have been observed upon oxidation of the film at low pH for the PAH-Os terminating layer. Moreover, at high pH values and with PVS as the terminating layer EQCM mass measurements have shown that cation release was masked by water exchange.

Introduction

Layer-by-layer ultrathin polyelectrolyte multilayer films can be prepared by sequential adsorption of oppositely charged polyelectrolytes from dilute aqueous solutions on charged solid substrates. Decher et al.[1−5] introduced a method to build uniform multilayers of polyelectrolytes by stepwise electrostatic adsorption between a charged surface and oppositely charged polymers in solution with molecular level control. Regulation of film thickness and restriction to a monolayer in each adsorption step can be easily achieved by repulsion of the soluble polymer of equal charge. Surface charge reversal operates in every immersion step.[6,7]

The layer-by-layer (LBL) electrostatic self-assembly (ESA) technique has been extended to a wide variety of materials including the following: synthetic polyelectrolytes,[8] proteins,[9] clay minerals,[10] dendrimers,[11] metal[12] and semiconductor colloidal particles,[13] dyes,[14] redox systems,[15] etc. As well, many applications have been found for the layer-by-layer electrostatic self-assembled films: enzyme active films,[16] permselectivity membranes,[17] selective patterning,[18] electrochromic,[19] light emitting diodes,[8,20] sensors,[21] nonlinear optics,[22] etc.

* Corresponding author. E-mail: calvo@q1.fcen.uba.ar.

(1) Decher, G. *Science* **1997**, *277*, 1232.
(2) Decher, G.; Hong, J. D.; Schmitt, J. *Thin Solid Films* **1992**, *210/211*, 831.
(3) Decher, G.; Hong, J. D. *Ber. Bunsen-Ges. Phys. Chem.* **1991**, *95*, 1430.
(4) Lvov, Y.; Decher, G.; Sukhorukov, G. *Macromolecules* **1993**, *26*, 5396.
(5) Lvov, Y.; Decher, G.; Mohwald, H. *Langmuir* **1993**, *9*, 481.
(6) Bertrand, P.; Jonas, A.; Laschewsky, A.; Legras, R. *Macromol. Rapid. Commun.* **2000**, *21*, 319.
(7) Arys, X.; Jonas, A. M.; Laschewsky, A.; Legras, R. *Supramolecular Polymers*; Ciferi, A., Ed.; Marcel Dekker: New York, 2000; pp 505−563.
(8) Shiratori, S. S.; Rubner, M. F. *Macromolecules* **2000**, *33*, 4213.
(9) Ladam, G.; Gergeli, C.; Seger, B.; Decher, G.; Voegel, J. C.; Schaaf, P.; Cuisinier, F. J. G. *Biomacromolecules* **2000**, *1*, 674.
(10) Kleinfeld, E. R.; Ferguson, G. S. *Science* **1994**, *265*, 370.
(11) (a) Watanabe, S.; Regan, S. L. *J. Am. Chem. Soc.* **1994**, *116*, 8855. (b) Yoon, H. C.; Hong, M. Y.; Kim, H. S. *Anal. Chem.* **2000**, *72*, 4420.
(12) Feldheim, D. L.; Grabar, K. C.; Natan, M. J.; Mallouk, T. C. *J. Am. Chem. Soc.* **1996**, *118*, 7640.
(13) Kotov, N. A.; Dekany, I.; Fendler, J. H. *J. Phys. Chem.* **1995**, *99*, 13065.
(14) Lvov, Y.; Decher, G. *J. Am. Chem. Soc.* **1997**, *119*, 2224.
(15) Cheng, L.; Niu, L.; Gong, J.; Dong, S. *Chem. Mater.* **1999**, *11*, 1465.
(16) (a) Onda, M.; Lvov, Y.; Ariga, K.; Kunitake, T. *Biotechnol. Bioeng.* **1996**, *51*, 163. (b) Hodak, J.; Etchenique, R.; Calvo, E. J.; Singhal, K.; Bartlett, P. N. *Langmuir* **1997**, *13*, 2716. (c) Calvo, E. J.; Etchenique, R.; Pietrasanta, L.; Wolosiuk, A.; Danilowicz, C. *Anal. Chem.* **2001**, *73*, 1161. (d) Calvo, E. J.; Battaglini, F.; Danilowicz, C.; Wolosiuk, A.; Otero, M. *Faraday Discuss.* **2000**, *116*, 47. (e) Lvov, Y.; Lu, Z.; Schenkman, J. B.; Zu, X.; Rusling, J. F. *J. Am. Chem. Soc.* **1998**, *120*, 4073. (f) Lvov, Y.; Ariga, K.; Ichinose, I.; Kunitake, T. *J. Am. Chem. Soc.* **1995**, *117*, 6117. (g) Sun, S.; Ho-Si, P. H.; Harrison, D. J. *Langmuir* **1991**, *7*, 727. (h) Mizutani, F.; Sato, Y.; Yabuki, S.; Hirata, Y. *Chem. Lett.* **1996**, 251. (i) Kinnear, K. T.; Monbouquette, H. G. *Langmuir* **1993**, *9*, 2255. (j) Guiomar, A. J.; Guthrie, J. T.; Evans, S. D. *Langmuir* **1999**, *15*, 1198. (k) Onda, M.; Lvov, Y.; Ariga, K.; Kunitake, T. *J. Ferment. Bioeng.* **1996**, *82*, 502. (l) Lvov, Y. *Protein Architecture*; Lvov, Y., Mohwald, H., Eds.; Marcel Dekker: New York, 2000; Chapter 6, p 125. (m) Blonder, R.; Katz, E.; Cohen, Y.; Itzhak, N.; Riklin, A.; Wilner, I. *Anal. Chem.* **1996**, *68*, 3151.
(17) (a) Harris, J. J.; Bruening, M. L. *Langmuir* **2000**, *16*, 2006. (b) Harris, J. J.; Stair, J. L.; Bruening, M. L. *Chem. Mater.* **2000**, *12*, 1941. (c) Stroeve, P.; Vasquez, V.; Coelho, M. A. N.; Rabolt, J. F. *Thin Solid Films* **1996**, *284/285*, 708. (d) Krasermann, L.; Tieke, B. *Langmuir* **2000**, *16*, 287.
(18) Hammond, P. T.; Whitesides, G. M. *Macromolecules* **1995**, *28*, 7569.
(19) (a) Stepp, J.; Schlenoff, J. B. *J. Electrochem. Soc.* **1997**, *144*, L155. (b) Laurent, D.; Schlenoff, J. B. *Langmuir* **1997**, *13*, 1552.
(20) (a) Eckle, M.; Decher, G. *Nanoletters* **2001**, *1*, 45. (b) Onitsuka, O.; Fou, A. C.; Rubner, M. F. *J. Appl. Phys.* **1996**, *80*, 4067.
(21) Sun, Y.; Zhang, X.; Sun, C.; Wang, B.; Shen, J. *Macromol. Chem. Phys.* **1996**, *197*, 147.
(22) (a) Balasubramamam, S.; Wang, X.; Wang, H. C.; Yang, K.; Kumar, J.; Tripathy, S. K.; Li, L. *Chem. Mater.* **1998**, *10*, 1554. (b) Laschewsky, V. *Thin Solid Films* **1996**, *284*, 334. (c) Lvov, Y.; Yamada, S.; Kunitake, T. *Thin Solid Films* **1997**, *300*, 107.

A number of ordered redox multilayers immobilized on modified electrode surfaces have been described.[23] Laurent and Schlenoff [19b] studied multilayer layer-by-layer assemblies of viologen polycation and PSS polyanion, where the redox centers through the multilayer structure are electrochemically addressable via electron hopping between neighboring sites. In these systems vectorial electron transfer and rectifying effects can be achieved. They showed some interpenetration of the polyions which has been confirmed by neutron reflectivity in similar structures.[24]

One of the most extensively studied LBL systems has been poly(allylamine), PAH, and poly(styrene-sulfonate), PSS, or poly(vinylsulfonate), PVS.[25] Our previous studies with ferrocene and osmium complexes covalently attached to poly(allylamine), respectively PAH-Fc[16b] and PAH-Os,[16c,d] have shown that in layer-by-layer nanostructures the enzyme glucose oxidase can be electrically connected ("wired") to an electrode surface with molecular recognition of glucose and generation of an electrical signal. In these systems we have found a systematic shift of the redox system peak potential dependence on the charge excess in the outermost layer in low ionic strength solutions.

The pioneering work of Anson[26] has shown that membrane or Donnan potential differences present at the interface between polyelectrolyte coatings on electrodes and the electrolyte solutions in which they are in contact contribute to the formal potentials measured for redox couples incorporated in the coatings such as Nafion. Doblhofer et al.[27] have shown that Donnan exclusion in the polyelectrolyte coatings exposed to electrolytic solutions results in a shift of the apparent formal potentials with electrolyte concentration. The interior of a swollen polymer coating may consist of Donnan domains where counterions are confined by electrostatic forces and regions filled by supporting electrolyte. Organized layer-by-layer polyelectrolytes containing redox groups are therefore attractive for studying the effect of Donnan potential on the redox potential shift as a function of the membrane surface charge and the mobile charge in solution.

Charge reversal upon adsorption of positively or negatively charged polyion on planar surfaces and colloidal particles has been reported for alternate layers. Negative ξ-potentials were observed when PSS was the outerlayer and positive ξ-potentials were measured for PAH as the outerlayer in colloidal particles modified with LBL ESA films[28,29] ($\xi = \pm 50$ mV approximately) while Decher[30] showed similar ξ-potentials on flat surfaces by studying streaming potentials.

It is generally assumed that the outermost layer, and not the underlying film, determines the surface potential.[28] However,

Knippel and co-workers studying the electrophoretic mobility of polystyrene-modified latex particles found that not only the top layer but also the layers underneath contribute to the particle mobility. They attributed this phenomena to incomplete coverage or polyelectrolyte interpenetration.[31]

The driving force for adsorption is mainly electrostatic, therefore charge density in the polymer, which depends on the ionic strength and solution pH for weak polyelectrolytes, plays a decisive role.

Donnan exclusion in self-assembled membranes composed of PAH and PSS affects anion transport in the multilayers.[17b,d] Recent studies with fluorescent probes assembled onto polyelectrolyte multilayer films on colloids showed that the multilayer systems may be described as Donnan systems with constant potential.[32] Also, metallopolyion films with in-film micelle formation in microemulsions develop a permselective barrier.[33]

In this paper we report redox potential shifts with ionic strength as a result of the Donnan potential set at the interface of the outermost region of the self-assembled layer and the electrolyte. We show Donnan permselectivity and ion exclusion in self-assembled redox polyelectrolyte multilayers affecting the electrochemical potential of redox probes embedded in the films. The redox potential of the osmium complex in the film is affected by the Donnan potential set primarily by the outermost charged region of the layer and the pH of the bathing solution.

To the best of our knowledge this is the first systematic study of Donnan potential effect on the apparent redox potential of a layer-by-layer self-assembled redox polyelectrolyte thin film. The dependence of the apparent redox potential shift for poly-(allylamine) derivatized with Os(bpy)$_2$ClPyCHO, PAH-Os, and poly(vinylsulfonate) (PVS), or poly(styrenesulfonate) (PSS) multilayers with the charge in the topmost layer, the electrolyte concentration, and solution pH is analyzed in terms of the Donnan equilibrium at the film/electrolyte solution interface due to the surface excess charge in the self-assembled multilayer.

Experimental Section

Poly(sodium 4-styrenesulfonate) salt (PSS, MW $\sim$ 70000, Aldrich), poly(vinyl-sulfonic acid) sodium salt (PVS, 25 wt % solution in water, Aldrich), and 3-mercapto-propanesulfonic, sodium salt (MPS, Aldrich) were used as received.

The redox polymer Os(bpy)$_2$ClPyCH$_2$NHpoly(allylamine) (PAH-Os) was synthesized as previously reported.[34]

Electrolyte solutions were prepared with Milli-Q (Millipore) water and reagents were used as received. The ionic strength of the solutions was adjusted with KNO$_3$.

Gold flags (0.5 × 1.0 cm^2) used as working electrodes were cleaned by immersion in fresh piranha (1:3 30% H$_2$O$_2$ and concentrated H$_2$-SO$_4$) solution for 20 min (**piranha solution is highly corrosive and reacts violently with organic materials: precautions must be taken at all times when handled**). Clean electrodes were rinsed with Milli-Q water and used immediately after cleaning. Before thiol adsorption the electrodes were cycled in 2 M sulfuric acid between 0.1 and 1.6 V at 0.1 V s^{-1} to check for surface contamination. Electrochemically active surfaces were calculated from the reduction peak of gold oxide.[35]

(23) Anicet, N.; Anne, A.; Moiroux, J.; Savéant, J. M. *J. Am. Chem. Soc.* **1998**, *120*, 7115.
(24) Lösche, M.; Schmitt, J.; Decher, G.; Bouwman, W. G.; Kjaer, K. *Macromolecules* **1998**, *31*, 8893.
(25) (a) Schmitt, J.; Grünewald, T.; Decher, G.; Pershan, P. S.; Kjaer, K.; Lösche, M. *Macromolecules* **1993**, *26*, 7058. (b) Lvov, Y.; Haas, H.; Decher, G.; Möhwald, H. *J. Phys. Chem.* **1993**, *97*, 12835. (c) Ferreira, M.; Rubner, M. F. *Macromolecules* **1995**, *28*, 7107.
(26) (a) Naegeli, R.; Redepening, J.; Anson, F. C. *J. Phys. Chem.* **1986**, *20*, 6227. (b) Ugo, P.; Anson, F. C. *Anal. Chem.* **1989**, *61*, 1802.
(27) (a) Doblhofer, K.; Armstrong, R. D.; Asturias, G. E.; Jang, G.; MacDiarmid, A. G.; Zhong, C. *Ber. Bunsen-Ges. Phys. Chem.* **1991**, *11*, 1381. (b) Doblhofer, K.; Vorotyntsev, M. *Electroactive Polymer Electrochemistry. Part 1. Fundamentals;* Lyons, M. E. G., Ed.; Plenum: New York, 1994; Chapter 3, p 375.
(28) Hoogeveen, N. G.; Stuart, M. A. C.; Fleer, G. J.; Bohmer, M. R. *Langmuir* **1996**, *12*, 3675.
(29) Caruso, F.; Donath, E.; Möhwald, H. *J. Phys. Chem. B* **1998**, *102*, 2011.
(30) Ladam, G.; Schaad, P.; Voegel, J. C.; Schaaf, P.; Decher, G.; Cuisinier, F. *Langmuir* **2000**, *16*, 1249.

(31) Donath, E.; Walther, D.; Shilov, V. N.; Knippel, E.; Budde, A.; Lowack, K.; Helm, C. A.; Möhwald, H. *Langmuir* **1997**, *13*, 5294.
(32) (a) Caruso, F.; Lichtenfeld, H.; Donath, E.; Möhwald, H. *Macromolecules* **1999**, *32*, 2317. (b) Sukhorukov, G. B.; Brumen, M.; Donath, E.; Möhwald, H. *J. Phys. Chem. B* **1999**, *103*, 6434.
(33) Njue, C. K.; Rusling, J. F. *J. Am. Chem. Soc.* **2000**, *122*, 6459.
(34) Danilowicz, C.; Corton, E.; Battaglini, F. *J. Electroanal. Chem.* **1998**, *445*, 89.

Scheme 1. Alternate Electrostatic Self-Assembly Procedure for Gold Electrodes
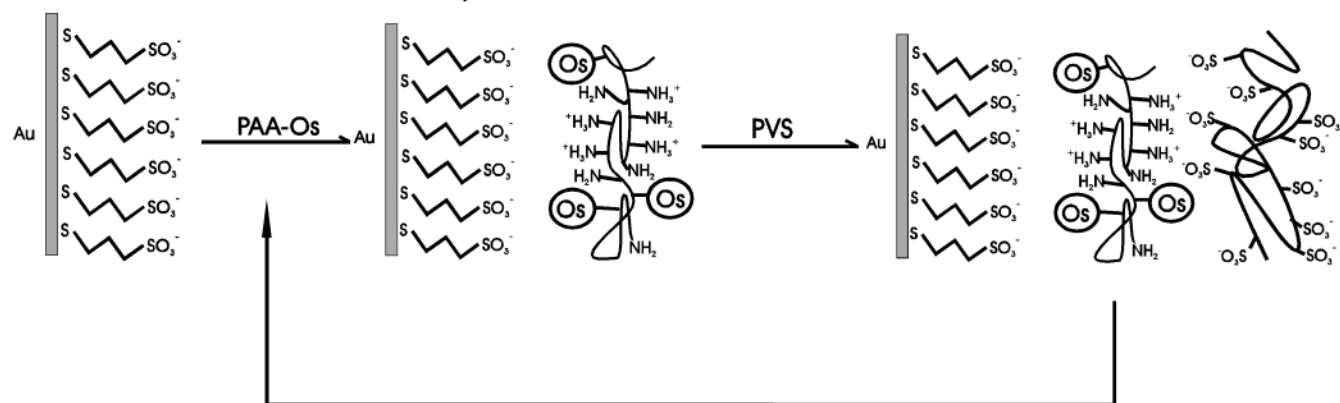
A standard three-electrode electrochemical cell was employed with a home-built operational amplifier potentiostat. The reference electrode was a saturated calomel electrode (SCE) and all potentials herein are quoted with respect to this reference; a platinum auxiliary electrode was employed.

Self-Assembly Process. (a) Thiol Adsorption. Thiol solutions were freshly prepared before each adsorption experiment to avoid oxidation in air. The MPS thiol monolayer was formed by soaking Au electrodes in aqueous solutions of 0.02 M sodium 3-mercapto-1-propane sulfonate in 0.01 M H_2SO_4 for 2 h. The Au samples were removed from the adsorption solution and thoroughly washed in distilled water.

(b) PAH-Os Adsorption. The poly(allylamine) osmium derivative was adsorbed on the thiol modified gold from 0.4% w/v aqueous solutions for 10 min. After adsorption the modified electrodes were thoroughly rinsed with distilled water.
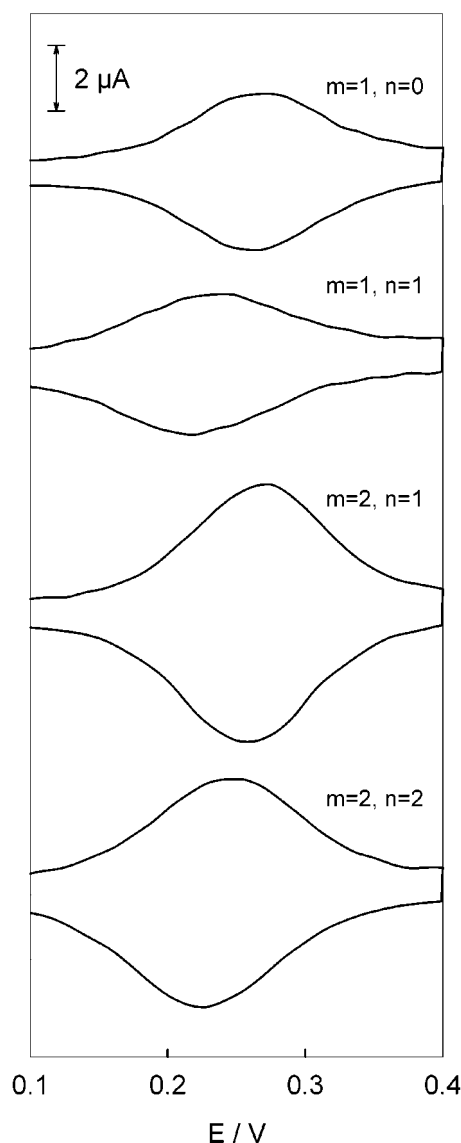
(c) PVS/PSS Adsorption. The polyelectrolytes were adsorbed onto the PAH-Os modified Au from 10 mg/mL aqueous solutions. After adsorption the modified electrodes were thoroughly rinsed with distilled water.

EQCM Experiments. Gold-coated Ti/Pd quartz crystals (ICM, Oklahoma City, OK, cat. 131392) with 10 nm Ti, 50 nm Pd, and 100 nm Au were used with an active area of 0.196 cm². Quartz crystal impedance measurements have been described elsewhere.[36]

Results and Discussion

1. Electrochemistry. Scheme 1 depicts the idealized scheme for the self-assembly process of PVS and PAH-Os on 3-mercaptopropane sulfonate (MPS) modified gold electrodes. A surface carrying a negative charge after adsorption of MPS was alternatively exposed to polyelectrolytes of different charge: poly(allylamine) with the Os complex covalently attached PAH-Os and poly(vinylsulfonate) (PVS) or polystyrene sulfonate (PSS) solutions in pure water. The process was repeated with water rinses between successive immersions so that the surface charge was reversed in each immersion in positively charged and negatively charged polymer and a multilayer was built by stepwise adsorption.

Figure 1 shows the cyclic voltammetry of a gold electrode modified with (PAH-Os)$_n$(PVS)$_n$ multilayers in 25 mM Tris-HCl buffer at pH 7.0. Behavior typical of a thin layer of electroactive material confined to a surface is observed;[37] however, the redox potential depends on the polyelectrolyte layer sequence (see below). We found reproducible cyclic voltammetries in 16 samples that were analyzed.
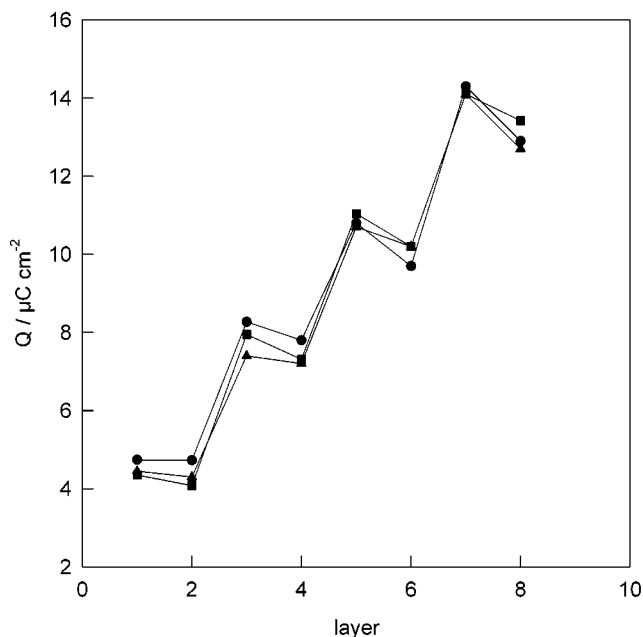
(35) Finklea, H. O.; Snider, D. A.; Fedyk, J. *Langmuir* **1990**, *6*, 371.
(36) Calvo, E. J.; Etchenique, R. *J. Phys. Chem. B* **1999**, *103*, 8944.
(37) Bard, A. J.; Faulkner, L. R. *Electrochemical Methods. Fundamentals and Applications*, 2nd ed.; Wiley: New York, 2001.

Figure 1. Cyclic voltammogram of (PAH-Os)$_m$(PVS)$_n$ with m, n = 1, 2 in 0.025 M Tris-HCl buffer at pH 7.0. ν = 0.05 V s^{-1}.

Figure 2 shows that the integrated charge increases when new layers of electroactive PAH-Os material are adsorbed. Little variation in redox charge was observed for different self-assembled electrodes (~10%). However, a small decrease is observed every time a negative layer (either PVS or PSS) is added. This decrease in redox charge may be due to some

Figure 2. Integrated redox charge for alternating layers of (PAH-Os)/(PSS) (●, 0.2 M ionic strenght) and (PAH-Os)/(PVS) (■, 0.2 M and ▲, 0.04 M ionic strength, respectively) in 0.04 M Tris-HCl buffer at pH 7.2.

Table 1. Fwhh for Different Electrostatically Self-assembled Structures[a]

	fwhh (mV) for PAH-Osm/PVSn		
m, n	*I* = 0.2 M	*I* = 0.04 M	*I* = 0.2 M
1, 0	104	111	110
1, 1	120	145	141
2, 1	107	115	126
2, 2	119	137	154
3, 2	107	113	126
3, 3	118	142	154
4, 3	104	114	131
4, 4	116	140	152

[a] Fwhh measured at 50 mV s^{-1} in 0.04 M Tris-HCl buffer at pH 7.2.

osmium polymer desorption from the surface into the electrolyte or to some hindrance of a fraction of the osmium sites for oxidation and reduction. Schlenoff et al.[38] have shown for similar systems with radiolabeled polyelectrolytes that there was no desorption of polymer from the surface when immersing the electrodes in solutions of the oppositely charged polyelectrolyte. The same behavior shown in Figure 2 has been seen in the electrostatic self-assembly process of charged enzymes or proteins over oppositely charged polymers.[16b–e] The amount of redox charge, obtained from the area under the anodic and cathodic peaks, increases with the number of redox layers; the peak height is proportional to the scan rate, indicating a fast electron-transfer process in the multilayer films with a constant number of redox sites accessible within the experimental time scale, ca. $\nu F/RT \approx 20-40$ s^{-1} (ν is the electrode potential scan rate, F is the Faraday constant, R is the gas constant, and T is the absolute temperature).

The full width at half-height (fwhh) is much larger than the value expected for an ideal one electron Nernstian redox system, ca. 90.6 mV with typical values between 100 and 160 mV indicative of repulsive interactions of the redox sites.[37] Most charges in the polyion film are intrinsically compensated; however, the local charge around the osmium redox centers may give rise to a distribution of formal potentials and rate constants.[39] It is noteworthy that the fwhh values also oscillate between two limits for positively and negatively charged terminated layers, respectively (see Table 1) and this variation is more important at low ionic strength. Therefore, we can conclude that the variation in the fwhh is of electrostatic nature.

The local electrostatic potential throughout the film thickness is expected to vary due to the distribution of positive and negative charges of the polyelectrolyte layers. The osmium

complex probes the local electrostatic potential and we should expect a distribution between two limiting charge environments (positively or negatively charge) around the redox centers. This redox population distribution would be responsible for the peak broadening, even if the film/electrolyte interface were neutral. Furthermore, the excess surface charge at the outermost polyion layer would give rise to strong electric fields which influence the polyion multilayer arrangement because the nonrigid structure can relax to a more even distribution of charge as demonstrated by Mohwald et al.[32a] Since the osmium redox couple is positively charged (either + or 2+) the asymmetric rearrangement due to either positive or negative surface charge excess would affect diferently the Os–Os site repulsive interactions and thus the voltammetry peak broadening.

The redox system Os(III)/Os(II) shows reversible behavior and symmetrical surface cyclic voltammetric waves are observed for both PVS and PSS films with a pronounced shift of the redox potential depending on the nature of the terminating layer: For positively charged PAH-Os capped films the $E^{1/2}_{app}$, taken as the midpoint between reduction and oxidation potential, is more positive than for negatively charged PVS or PSS terminated layers.

The structural difference between PVS and PSS is that poly-(styrene) sulfonate is a more rigid polymer due to the aromatic rings; however, the effect of the charged terminal layer is similar in both cases. This suggests that the redox potential and the fwhh for the Os polymer films are modulated by the charge excess in the outermost layers in the multilayer film, which reverts in every adsorption step.

Figure 3 depicts the apparent redox formal potential values observed as a function of the polyelectrolyte layer number for PAH-Os and PVS or PSS multilayer coated electrodes. In all cases a shift of the redox potential for consecutive layers is observed with a larger magnitude of the potential shift at low ionic strength. At a given ionic strength the redox potential alternates between two limiting values for the positively charged and negatively charged top layer, respectively. For 0.2 M background electrolyte the redox potential shift amounts to some 40 mV, while for 0.04 M the potential oscillation reaches almost 100 mV. These magnitudes are comparable to the ζ-potential shifts observed for alternate adsorption of similar polyelectrolytes on electrode surfaces[30] and on colloid surfaces.[28,29] Similar alternating properties with a reverse in the polyelectrolyte surface charge have been reported in related ESA systems for contact angle,[40] ellipsometric angles,[41] electrophoretic mobility,[28,29] etc.

(38) Schlenoff, J. B.; Ly, H.; Li, M. *J. Am. Chem. Soc.* **1998**, *120*, 7628.
(39) (a) Albery, W. J.; Boutelle, M. G.; Colby, P. J.; Hillman, A. R. *J. Electroanal. Chem.* **1982**, *141*, 135. (b) Nahir, T. M.; Bowden, E. F. *J. Electroanal. Chem.* **1996**, *410*, 9.

(40) Yoo, D.; Shiratori, S. S.; Rubner, M. F. *Macromolecules* **1998**, *31*, 4309.
(41) Ruths, J.; Essler, F.; Decher, G.; Riegler, H. *Langmuir* **2000**, *16*, 8871.
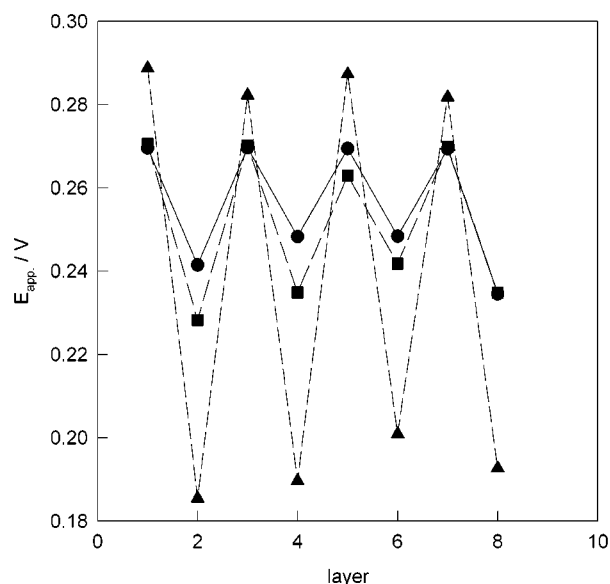
Figure 3. Redox potential as a function of layer number and total ionic strength for (PAH-Os)/(PSS) (●, 0.2 M) and (PAH-Os)/(PVS) (■, 0.2 M and ▲, 0.04 M) in 0.04 M Tris-HCl buffer at pH 7.2.
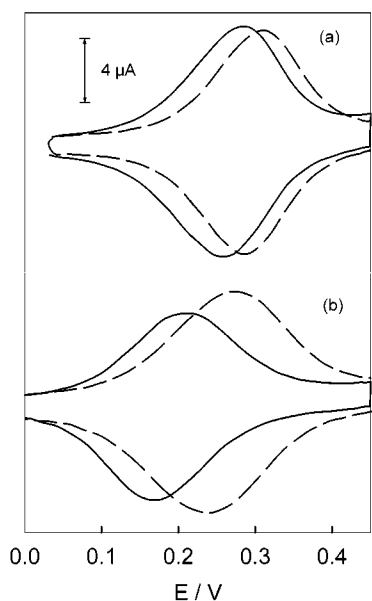
Figure 4. Cyclic voltammograms of (a) (PAH-Os)$_5$(PVS)$_4$ and (b) (PAH-Os)$_5$(PVS)$_5$ in solutions of 0.025 M acetic acid/acetate buffer pH 4.0 (- - -) and 0.025 M Tris buffer at pH 7.5 (—) at 0.05 V s^{-1}. The total ionic strength in both solutions was 0.04 M.

Figure 4 shows the effect of solution pH on the cyclic voltammograms of (PAH-Os)$_n$(PVS)$_n$ multilayers at constant ionic strength. An increase in solution pH results in a shift of $E^{1/2}_{app}$ to less positive values in all cases. For PAH-Os terminated layers the higher pH produces a film with less surface positive charge due to deprotonation of NH$_3^+$ groups. At pH 4 NH$_2$ groups in poly(allylamine) are almost all protonated while at pH 7 only 70−60% of these groups are protonated.[42] Note that for negatively charged PVS terminated layers (Figure 4b) less positive $E^{1/2}_{app}$ are observed at a given pH than for positively charged PAH-Os capped films (Figure 4a).

A qualitative analysis of the shift in $E^{1/2}_{app}$ in the negative direction relates the observed effect to a decrease of surface

(42) Yoshikawa, Y.; Matsuoka, H.; Ise, N *Br. Polym. J.* **1986**, *18*, 242.

Table 2. Cyclic Voltammetry Parameters of Figure 4a,b

	$Q/\mu C\ cm^{-2}$	$E^{1/2}_{app}/V$		fwhh/mV	
		pH 4	pH 7	pH 4.0	pH 7.0
(PAH-Os)$_5$(PVS)$_4$	16.0	0.303	0.270	124	120
(PAH-Os)$_5$(PVS)$_5$	15.5	0.255	0.190	146	156

positive charge or an increase in negative surface charge of the topmost assembled layers. Table 2 summarizes these results: While the redox charge of these films is nearly constant the peak width (fwhh) is larger for PVS terminated layers. Deprotonation of PAH-Os capped films results in a slight variation of fwhh. On the other hand, when PVS is the terminating layer the fwhh increases with pH rise. This behavior suggests that negative charges in the film may induce a broader distribution of formal potentials.[39] The shift in the redox potential is larger for the PVS top layer ($\Delta E^{1/2}_{app} = 65$ mV) than for the PAH-Os capped layer ($\Delta E^{1/2}_{app} = 33$ mV).

The effect of the electrolyte pH on the $E^{1/2}_{app}$ shift is larger for low ionic strength and negligible at 1 M, due to screening of surface charge by the electrolyte (see Figure 2, Supporting Information). A strong effect of the electrolyte pH on the apparent redox potential is observed at low constant ionic strength due to the protonation of the NH$_2$ groups in the weak polyelectrolyte PAH, and thus modulation on the fixed charge in the polymer backbone. The higher the pH the less positively charged the film and therefore the $E^{1/2}_{app}$ shifts to less positive potentials.

At constant pH the increase in ionic strength results in a shift of the redox potential in the direction of the soluble osmium complex redox potential, ca. $E^{o\prime} = 0.25$ V.[34] Peak broadening (fwhh) decreases at higher ionic strength due to charge screening by the electrolyte while the redox charge is almost constant.

The partition of ions between bathing electrolyte solution and films with fixed charges such as Nafion has been extensively studied.[26,27]

Assuming for simplicity that there is no change in the resolvation energy of the ions in the solution and inside the film ($\Delta \mu_i^o = 0$) and that they have the same activity coefficients, $\gamma_i^{film} = \gamma_i^{soln}$, a potential across the interface develops, the Donnan potential, $\Delta \phi_D$:[27b]

$$\Delta \phi_D = \frac{\omega RT}{F} \ln \left[\frac{c_F + (c_F^2 + 4c_S^2)^{1/2}}{2c_S} \right] \qquad (1)$$

where c_S is the 1:1 electrolyte concentration in the external solution, c_F is the concentration of fixed charged sites in the polymer, and ω is the ionic charge of the fixed ionic sites in the polymer.

The effect of electrolyte concentration and pH on the resulting Donnan potential predicted by eq 1 is shown in Figure 5 with plots simulated using eq 1 with $c_F = 0.1$ to 5 M and $\omega = 1$. The plots of $\Delta \phi_D$ vs log c_S (in the range 1 mM to 2 M) show a linear decrease in $\Delta \phi_D$ increasing the electrolyte concentration until Donnan breakdown is reached at high electrolyte concentration.

For PAH the fixed charge in the NH$_3^+$ groups in the polyelectrolyte is a function of pH, according to the surface acid−base equilibrium:[42]
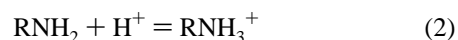
$$RNH_2 + H^+ = RNH_3^+ \qquad (2)$$
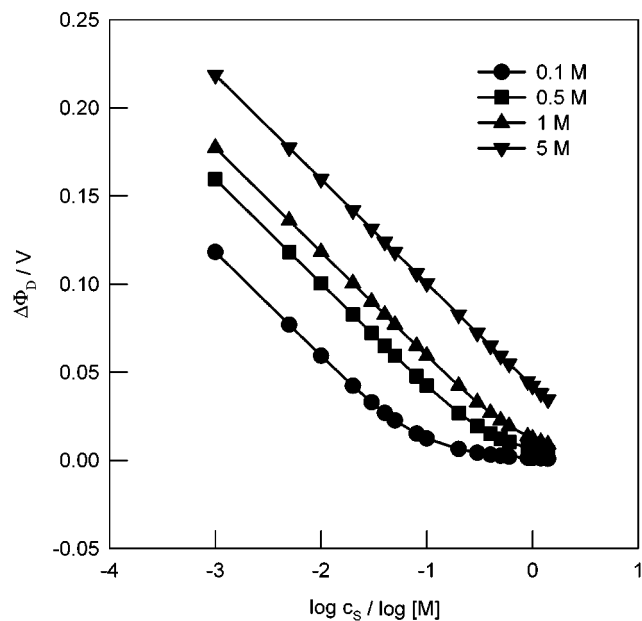
Figure 5. Donnan potential calculated with eq 1 vs log c_S for different concentrations of fixed charge in the PAH polyelectrolyte film (0.1 to 5 M) for $\omega = 1$.

The increase in the concentration of fixed charges in the polymer film c_F at lower pH for PAH-Os extends the Donnan exclusion region to higher electrolyte concentration.

It is worthwhile noticing that for $c_S \ll c_F$ in eq 1 Donnan permselectivity applies and a contribution of approximately 60 mV per 10-fold c_S in the Galvani potential difference is expected:
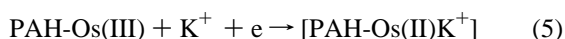
$$\Delta\phi_D \approx \omega \frac{RT}{F}\ln\frac{c_F}{c_S} \qquad (3)$$

This can be rationalized with the reaction:

$$X[\text{PAH-Os(III)}] + e^- \rightarrow \text{PAH-Os(II)} + X^- \qquad (4)$$
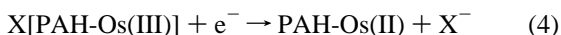
where X^- represents an anion in the electrolyte.

Conversely, eq 4 can be rewritten as:

$$\text{PAH-Os(III)} + K^+ + e \rightarrow [\text{PAH-Os(II)}K^+] \qquad (5)$$

if a cation K^+ is incorporated into the polymer film upon reduction (for $\omega = -1$).

Similar reactions have been studied on polymer modified electrodes and constitute a basis for potentiometric sensors.[26,27b,32b,33]

The apparent redox potential of the modified electrode with respect to the reference electrode is given by $E^{1/2}_{app} = E^{o\prime} + \Delta\phi_D$, where $E^{o\prime}$ is the formal redox potential of the Os(III)/Os-(II) redox couple in the absence of electrostatic work terms due to the charged polymer.

Figure 6 depicts curves of $E^{1/2}_{app}$ versus log c_S for data at pH 9.2 and 5.0 for (PAH-Os)$_4$(PVS)$_4$. The solid lines are the best fit lines to eq 1 and the values of $c_F = 52$ mM and $E^{o\prime} = 0.260$ V (pH 9.2) and $c_F = 290$ mM and $E^{o\prime} = 0.265$ V (pH 5.0) result from the respective curve fitting process. It is worthwhile noticing the good coincidence of the formal redox potential at the Donnan breakdown when the electrostatic effects are completely shielded. At pH 5 PAH has almost all its NH$_2$
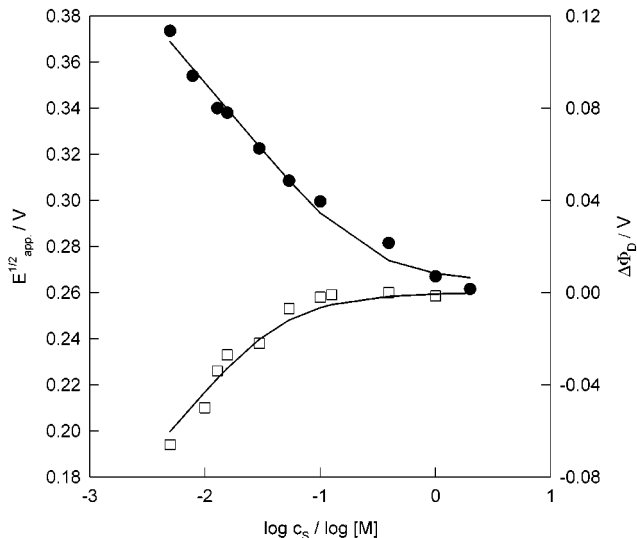
Figure 6. Variation of formal potential for a self-assembled (PAH-Os)$_4$-(PVS)$_4$ film in KNO$_3$ solutions of different ionic strength (c_S) and different pH: (●) 5.0 and (□) 9.2. Calculated $\Delta\phi_D$ using eq 1 and $E^{o\prime} = 0.26$ V for Os(bpy)$_2$ClPyCHO.

groups protonated and the negative slope of the Donnan potential vs log c_S plot implies anion exchange, thus cation exclusion. At pH 9.2, on the other hand, cation exchange is apparent from the positive slope in Figure 6 with expulsion of cations from the film upon Os(II) oxidation.

The results shown so far demonstrate that the major contribution to the mechanism of ion exchange during redox switching depends mainly on the charge in the film, i.e., the sign of the Donnan potential: the negative slope indicates exchange of anions ($\omega = 1$) and the positive slope exchange of cations ($\omega = -1$).

The anion exchange at pH 5.0 for (PAH-Os)$_4$(PVS)$_4$ with negatively charged PVS as the topmost layer (Figure 6) arises from the protonation of PAH at low pH decreasing the surface negative charge due to PVS groups fixed to the surfaces by ion pair formation.[31]

For a positively terminated film (PAH-Os)$_5$(PVS)$_4$ with an extra PAH-Os layer with respect to (PAH-Os)$_4$(PVS)$_4$, on the other hand, we find anion permselectivity for both pH 5.0 and 9.2, with $c_F = 320$ mM and $E^{o\prime} = 0.261$ V and $c_F = 100$ mM and $E^{o\prime} = 0.250$ V, respectively, as shown in Figure 7.

A sharp potential drop at the film–electrolyte interface is not to be expected since it is known that self-assembled polymer layers interpenetrate to some extent (on average 4 layers[1,19b]) leading to a smooth potential gradient at the film–electrolyte interface with participation of the underneath layers in the surface charge balance.

Measuring the electrical charge density consumed during the oxidation of Os(II) to Os(III) and assuming a bilayer thickness of 2 nm[31] an estimate of the osmium sites concentration can be made. As the PAH is modified in a 1:10 ratio with the Os complex, the total concentration of positive charges is in the 1–1.5 M range. However, given that there is a certain degree of intrinsic compensation of charges within the multilayer,[31,32,38,39] c_F represents the excess concentration of charges. Caruso and co-workers demonstrated for PAH/PSS systems that a minimum of 10–30% of total cationic charges were not involved in ion-pair binding.[32a] The c_F values obtained for PAH-
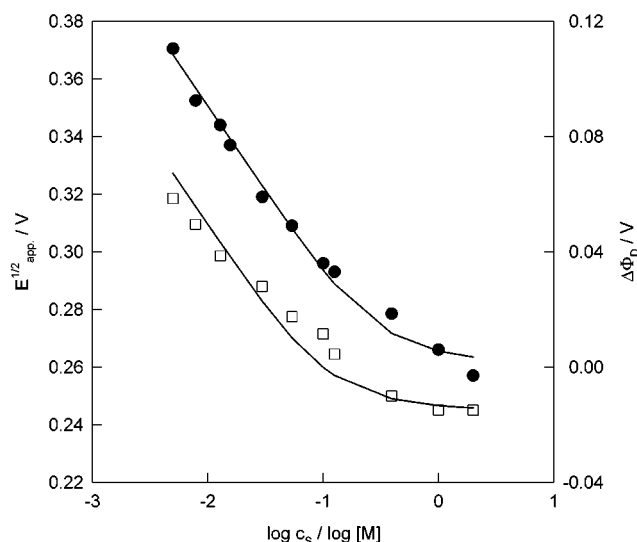
Figure 7. Variation of the formal potential for a self-assembled (PAH-Os)$_5$(PVS)$_4$ film in KNO$_3$ solutions of different ionic strength (c_S) and different pH: (●) 5.0 and (□) 9.2. Calculated $\Delta\phi_D$ using eq 1 and $E^{\circ\prime} = 0.26$ V for Os(bpy)$_2$ClPyCHO.

Os capped films agree reasonably well with their observations.

The apparent redox potential of PAH-Os polyelectrolyte in electrostatically self-assembled layers with PSS as the polyanion also shifts toward lower values at higher supporting (1:1) electrolyte concentration with a negative slope in $E^{1/2}_{app}$ vs log c_S plots for 10 mM to 0.1 M (Donnan permselectivity). Beyond $c_S = 0.5$ M, Donnan breakdown is also apparent with the ingress of salt in the thin polyelectrolyte film.

2. Quartz Crystal Microbalance. Electroneutrality in the film requires that the amount of charge introduced in the polymer layers by oxidation of Os(II) needs to be balanced by anion uptake or cation expulsion. From the dependence of the formal redox potential with the electrolyte concentration we have shown that exchange of ions occurs under permselectivity conditions and Donnan breakdown takes place when the electrolyte concentration exceeds the ionic charge in the polymer, c_F, and then salt can be exchanged. In addition to that, the ionic exchange usually involves the exchange of solvent. Both ion and solvent fluxes can be monitored by the resonant frequency shift of the quartz crystal microbalance, Δf_s. However, the use of the EQCM in water to measure mass variations in self-assembled films is limited by the intrinsic viscoelastic attenuation of the shear wave. Quartz crystal impedance analysis [36] allows the change in dissipation resistance in addition to the resonant frequency, ΔR, to be followed as the electrochemical process takes place. In the system reported here, $\Delta R \sim 0$, so if $\Delta f_s \ll f_s$ the Sauerbrey equation [43] applies:

$$\Delta f_s = -\frac{2f_s^2}{\sqrt{\mu_Q \rho_Q}} \frac{\Delta m}{A} \qquad (6)$$

with f_s the fundamental resonant frequency of the quartz crystal, Δm the mass loading, A the piezoelectrically active area, ρ_Q the quartz density (2.648 g cm^{-3}), and μ_Q the shear modulus of AT-cut quartz (2.947 × 10^{11} dyn cm^{-2}). The sensitivity factor for an AT-cut 10 MHz quartz crystal is 0.226 Hz cm^2 ng^{-1}.

(43) Sauerbrey, G. *Z. Phys.* **1959**, *155*, 206.
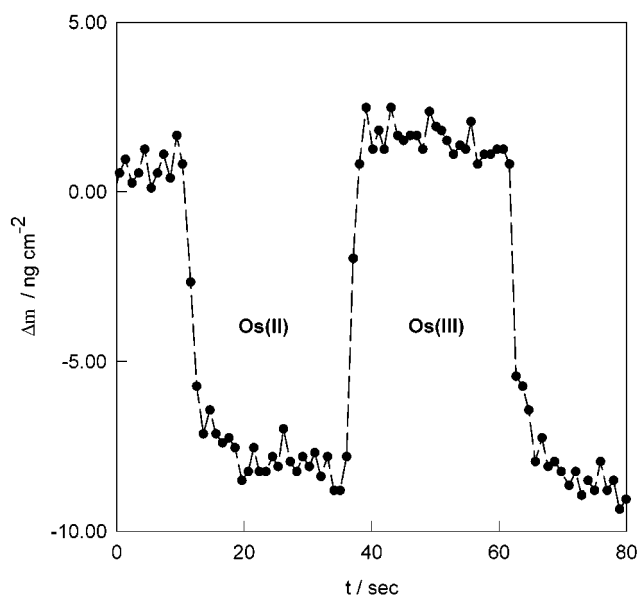
Figure 8. Mass variation with redox state for a self-assembled (PAH-Os)$_{10}$(PVS)$_{10}$ film in 10 mM HEPES buffer at pH 6.8 and 1 M KNO$_3$.
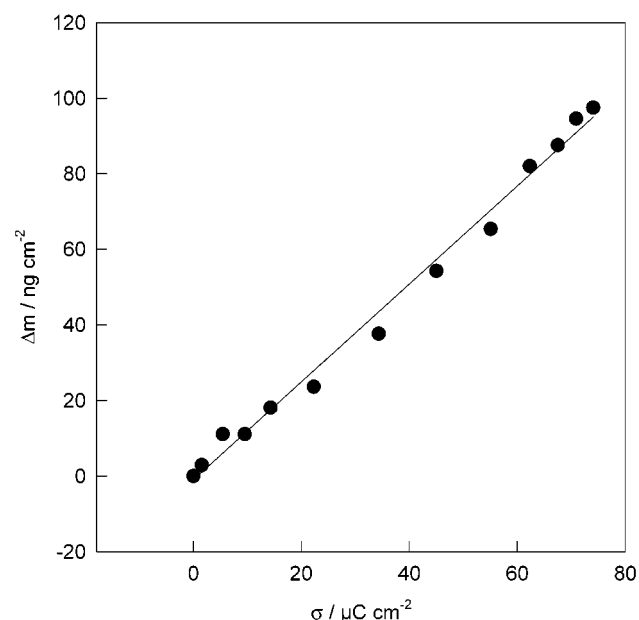
Figure 9. EQCM mass increment with faradic charge for a self-assembled (PAH-Os)$_{10}$(PVS)$_{10}$ electrode in 10 mM HEPES buffer at pH 6.8 and 1 M KNO$_3$.

To monitor the exchange of ions and solvent during the electrochemical oxidation, a Ti/Pd Au coated quartz crystal was modified with (PVS)$_{10}$(PAH-Os)$_{10}$ and the resonance frequency recorded simultaneously to the electrochemical oxidation−reduction of the film. The variation of mass calculated from the resonant frequency shift with the Sauerbrey equation [43] is shown in Figure 8 for a potential step from the fully oxidized to the fully reduced PAH-Os film between 0.4 and 0.04 V. An increase in mass is apparent during oxidation while reduction of Os(III) produces a decrease in mass.

In Figure 9 we compare the mass gain during film oxidation with the quantity of oxidation charge. A linear mass-to-charge relationship is apparent with a slope that results in a calculated molar mass for the exchanged species of 120 g mol^{-1} under Donnan breakdown for 1 M KNO$_3$ at pH 6.8 (see Figure 6).

Table 3. Mass Exchange Detected by EQCM[a]

	Δm/g mol^{-1}		
ionic strength/M	pH 9.2	pH 6.8	pH 4.4
1	128	120	101
0.3	32	60	b
0.075	25.6	60	89

[a] Exchanged molecular mass in self-assembled electrode (PAH-Os)$_{10}$(PVS)$_{10}$ in HBO$_3$/BO$_2^-$ buffer (pH 9.2), HEPES (pH 6.8), and acetic/acetate (pH 4.4) with increasing concentration of KNO$_3$ (M_{K^+} = 39 g mol^{-1} and $M_{NO_3^-}$ = 62 g mol^{-1}). [b] Not measured.

The molar mass of the NO$_3^-$ anion and the K$^+$ cation is 62 and 39 g mol^{-1}, respectively, so we conclude that water must be incorporated into the film in addition to the salt under those conditions.

At lower ionic concentration and the same pH, however, under Donnan anion permselectivity we find 60 g mol^{-1} so that only nitrate and no solvent is exchanged. Table 3 compiles the molar masses for other pH values and electrolyte concentrations.

At high pH (low fixed charge in PAH-Os) and low ionic strength the exchanged mass per Faraday is less than the anion or cation molecular weight. Under Donnan breakdown conditions, on the other hand, salt and water are exchanged with a larger mass gain, ca. 128 g mol^{-1}. Charge compensation by cation elimination from the film during oxidation of the negatively charged topmost layer under permselective conditions should result in a decrease of 39 g mol^{-1} per Faraday. In contrast the EQCM detects an increase 25−30 g mol^{-1} per Faraday and therefore we conclude that simultaneous to the loss of the cation an important ingress of solvent must occur.

At lower pH (larger fixed positive charge in PAH-Os) and under permselectivity conditions the EQCM shows an exchanged molar mass close to that expected for nitrate ion, which is evidence of anion exchange during (PAH-Os)$_{10}$(PVS)$_{10}$ redox switching. For Donnan breakdown, above 1 M electrolyte concentration both water and anions or salt are exchanged since the exchanged species molar mass exceeds 100 g mol^{-1}.

Conclusions

The nature of the polyelectrolyte capping layer, the electrolyte pH, and ionic strength determine the apparent redox potential of the osmium couple in the film, $E^{1/2}_{app}$, due to the self-assembled layer surface charge. This phenomenon is related to the well-known shift in ξ-potential shift of LBL self-assembled flat surfaces and colloidal particles.[28−31]

The redox potential dependence on electrolyte ionic strength can be described by Donnan exclusion by the fixed charge of polyions in the film. The fixed charges are given by the PAH-Os (pH dependent) and PSS or PVS (pH independent) charge density in the polyion segments. The LBL technique allows control of the net charge density of the film and also its permselectivity. Previous work done over modified polymer electrodes was based on thick films with a random distribution of its components.[26,27] The fine-tuning of the LBL assembly permits nanometer scale modification of surfaces with important changes in the film properties.

For PAH-Os polycation capped films the ingress of anions to maintain electroneutrality within the films has been observed during Os(II) oxidation under permselectivity conditions (low ionic strength and low pH). At high electrolyte concentration Donnan breakdown occurs above 0.5 M.

For negatively charged PSS or PVS capped films cation exchange has been found for high pH and low ionic concentration. However, at low pH cation exclusion is observed due to the overcompensation of PSS or PVS charge in the topmost layer of the film by the underneath protonated PAH-Os layers.

The EQCM has shown that under cation exclusion conditions only anions are exchanged during the redox switching for low ionic concentration while for Donnan breakdown both water and anions exchange has been detected. When the topmost layer is negatively charged (PSS or PVS), under cation permselective conditions the egress of cations during Os(II) oxidation is masked by the ingress of solvent.

Supporting Information Available: Succesive cyclic voltammetries of (PAH-Os)$_n$(PSS)$_n$ following the build-up process; cyclic voltammetries of (PAH-Os)$_6$(PVS)$_6$ in solutions of different pH variable ionic strenght (PDF). This material is available free of charge via the Internet at http://pubs.acs.org.

JA020107H